Available online at www.sciencedirect.com

SciVerse ScienceDirect

Scripta Materialia 67 (2012) 5–8

Scripta MATERIALIA

www.elsevier.com/locate/scriptamat

Matrix-controlled morphology evolution of Te inclusions in CdZnTe single crystal

Yihui He, Wanqi Jie,* Yadong Xu, Tao Wang, Gangqiang Zha, Pengfei Yu, Xin Zheng, Yan Zhou and Hang Liu

State Key Laboratory of Solidification Processing, Northwestern Polytechnical University, Xi'an 710072, China

Received 23 December 2011; revised 21 February 2012; accepted 5 March 2012
Available online 9 March 2012

The fine morphologies of microscale Te inclusions in CdZnTe single crystal were investigated to reveal their shape evolution. Such inclusions from crystal ingots with different post-growth cooling rates were analyzed using scanning electron microscopy after surface treatment. A tetrakaidecahedron model embodying {1 0 0} and {1 1 1} matrix facets was developed to interpret the form of the Te inclusions. An entire shape evolution process was also proposed where the final configuration of the Te inclusions was a tetrahedron comprising {1 1 1}B facets.

Keywords: Compound semiconductors; Scanning electron microscopy (SEM); Surface energy (anisotropy); Precipitation crystallography; Shape evolution

$Cd_{0.9}Zn_{0.1}Te$ (CZT) has been proven to be the most promising material for hard X- and γ-ray detection at room temperature [1], complementary to scintillators and liquid nitrogen-cooled high-purity germanium (Ge) or silicon (Si) detectors [2,3]. CZT crystals grown under a slight excess of tellurium exhibit high resistivity due to the formation of Te antisites [4]. However, the inevitable constitutional supercooling during melt growth of such a multi-component system may cause the solid–liquid interface to transform from planar to cellular, leading to the trapping of Te-rich melt in the matrix [5]. Subsequently, the Te inclusions will form facets surrounded by CZT crystals during an isothermal in situ annealing and cooling process. A high density of Te inclusions embedded in the matrix may even induce extended defects, such as dislocations or stress [6], which will trap the activated charges and thus reduce the efficiency of the detector [7]. Furthermore, gliding patterns of dislocations induced by them may be related to the shape of the inclusions [8].

Over the past few decades, considerable efforts have been made to understand the formation of Te inclusions and their various morphologies under different growth conditions [9–11]. As yet, however, only speculative explanations for the variety of shapes evident have been given [12]. To explain the final shape of Te inclusions, Rudolph et al. [9] suggested that Te-rich droplets might be trapped in a regular negative polyhedron in the solid–liquid interface. However, considering that the final morphology of Te inclusions is completely changed from that at the beginning of their formation, such a speculation may not be able to explain the experimental results. Though many studies have looked at the morphological evolution from a variety of aspects [10,11,13], the entire process is still an open question. In the present work, we focus on the morphology of Te inclusions so as to reveal their shape evolution process with regard to growth conditions.

A special surface treatment was employed to reveal the form of the Te inclusions; this is described in detail in the Supplementary Data. Prior to the etching of the interface between the Te inclusions and the CZT matrix, the contour of the Te inclusions is revealed on the surface, as indicated in Figure 1. Electron probe composition analysis reveals that Te inclusions are almost pure tellurium (>99 at.%), with negligible cadmium and zinc. The cubo-octahedron-shaped Te inclusion in Figure 1a is exposed on the wafer surface after etching. Figure 1b–d shows Te inclusions with different cross-sections on {1 1 1} faces. Due to the relatively high etching rate of Everson's solution, several micrometers of CZT material

---

* Corresponding author. Tel.: +86 29 88460445; fax: +86 29 88495414; e-mail: jwq@nwpu.edu.cn

1359-6462/$ - see front matter Crown Copyright © 2012 Published by Elsevier Ltd. on behalf of Acta Materialia Inc. All rights reserved.
http://dx.doi.org/10.1016/j.scriptamat.2012.03.008

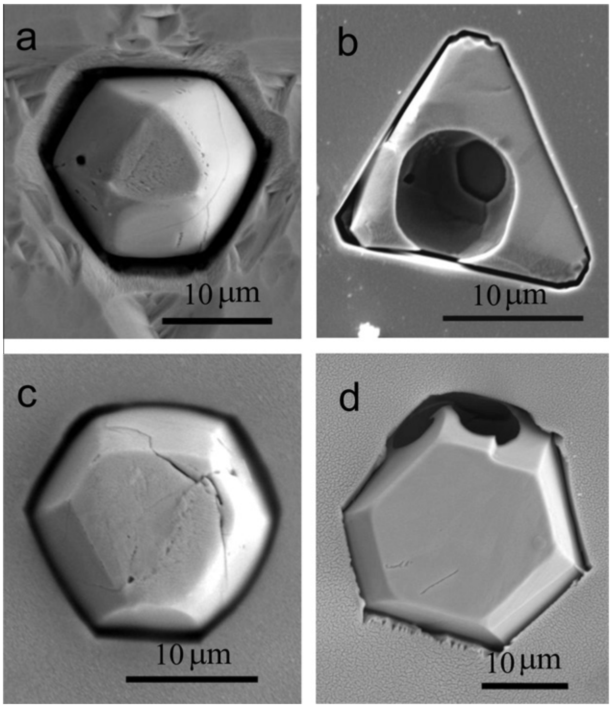

Figure 1. Te inclusions observed on etched CZT surfaces. (a) A cubo-octahedral Te inclusion on a {1 1 1}B face etched by Everson's solution. (b) A triangular Te inclusion on a surface chemically polished with 2% bromine in methanol solution. (c, d) Hexagonal Te inclusions on {1 1 1}A faces etched by Everson's solution.

below the original surface layer was removed and the Te inclusions were exposed. In addition, as the thermal expansion coefficient of tellurium is significantly higher than that of CZT, voids are often observed, which usually remain spherical for the minimum of surface energy, as shown in Figure 1b and d.

Figure 2a–d shows some well-defined cavities left by Te inclusions following the special surface treatment. The morphologies of the Te inclusions are expected to be equivalent to those of the cavities. Figure 2a shows a complex polyhedron cavity encompassed by triangular and square facets. The cavity in Figure 2b shows three-fold symmetry. Figure 2c shows a tetrahedral cavity obtained by cutting six edges of a truncated tetrahedron, which is comparable to the suggestion of Rudolph et al. [9], who considered that Te inclusions were embedded in a cavity formed initially by two adjacent truncated tetrahedrons comprising {1 1 1} faces. Analogous morphologies have often been prepared in the synthesis of nanoparticles [14,15].

Based on these observations, we propose a tetrakaidecahedron (14-hedron) model, embodying six {1 0 0} and eight {1 1 1} facets, to interpret the form of the Te inclusions or cavities, as shown in Figure 2e–h. The models were obtained using the computer program WinXMorph [16]. The crystallographic plane of the model represents the surface of the cavities. Here, the model can be defined as a function of the shape factor R, viz $R = d\{100\}/d\{111\}$, where $d\{100\}$ and $d\{111\}$ are the distances from the centroid of the polyhedron to the {1 0 0} and {1 1 1} faces, respectively. The shape factor R can reflect the macroscopic shape of the Te inclusions, and the growth rate of the different faces to some extent. The typical shape of the Te inclusions or cavities with $R = 0.87$ is a cubo-octahedron, as shown in Figure 2e, while the shape of those with $0.87 > R > 0.58$ is a truncated hexahedron, as shown in Figure 2h. It is worth noting that there is no single shape factor R in Figure 2f and g, owing to the remarkable enlargement of the {1 1 1}B faces. Additional experiments have been performed to confirm the above models and to ascertain the increscent faces through an indirect approach, as indicated in the Supplementary Data. Moreover, such tetrahedral inclusions have been found to be abundant in CZT crystal, especially in the first freezing part of the crystal ingot. This variety of shapes implies that an evolutionary process may occur during the post-growth cooling and the polarity of the {1 1 1} faces may play a special role in defining the morphology of the Te inclusions.

Generally, Te droplets captured by the solid–liquid interface undergo a slow solidification process, during which partial CZT dissolved in the droplets will separate out and planes with low interfacial energy will show. To refine this evolution mechanism and the final equilibrium form of the Te inclusions, we discuss this further qualitatively.

From the kinetics aspect, factors such as the cooling rate would have a significant impact on the evolution stages of the captured Te droplets during cooling. The volume of Te inclusions is also a key factor dominating the rate of shape change.

A series of infrared transmission microscopic images of Te inclusions obtained under different cooling rates after crystal growth are shown in Figure 3 in the Supplementary Data. When the cooling rate is lower than 5 K h^{-1}, Te inclusions with an average diameter of <30 μm tend to form as tetrahedrons, while those of 30–50 μm form truncated tetrahedrons. As the cooling rate increases to 10 K h^{-1}, Te inclusions of <20 μm have already formed as tetrahedrons, but the larger ones, in the range of 30–50 μm, keep their cubo-octahedron configuration. Therefore, Te inclusions are more inclined to form tetrahedrons when the cooling rate is slower.

Isothermal annealing of the crystal before cooling to room temperature relaxes the stress and redistributes the point defects. Long-term annealing also caused Ostwald ripening of the Te inclusions [17]. Owing to the rapid cooling rate, ~50 K h^{-1}, the Te inclusions are probably not able to crystallize anisotropically but maintain the ripening shape, as shown in Figure 3 in the Supplementary Data. In such a case, the distortion produced by deformation of the matrix lattice is usually severe [12], and the defects, e.g. dislocation loops, gathered around the interface will probably induce deep-level traps or carrier recombination centers, which would reduce the transport properties of the crystal [18].

Furthermore, for a specific CZT ingot with an intermediate cooling rate of ~10 K h^{-1}, a statistical relationship between the volume and the $S\{111\}/S\{100\}$ ratio of cavities is also obtained, as shown in Figure 3. As indicated in the figure, the ratio follows a pronounced exponential attenuation with increasing volume, which may be related to the solute diffusion and precipitation process inside the droplets during cooling. Specifically,